Universal sequence of ordered structures obtained from mesoscopic description of self-assembly

A. Ciach
Institute of Physical Chemistry, Polish Academy of Sciences, 01-224 Warszawa, Poland
(Received 17 September 2008; published 19 December 2008)

Mesoscopic theory for soft-matter systems that combines density functional and statistical field theory is derived by a systematic coarse-graining procedure. For particles interacting with spherically symmetric potentials of arbitrary form, the grand-thermodynamic potential consists of two terms. The first term is associated with microscopic length-scale fluctuations, and has the form of the standard density functional. The second term is associated with mesoscopic length-scale fluctuations, and has the form known from the statistical field theory. For the correlation function between density fluctuations in mesoscopic regions, a pair of equations similar to the Ornstein-Zernicke equation with a new closure is obtained. In the special case of weak ordering on the mesoscopic length scale, the theory takes a form similar to either the Landau-Ginzburg-Wilson (LGW) or the Landau-Brazovskii (LB) field theory, depending on the form of the interaction potential. Microscopic expressions for the phenomenological parameters that appear in the Landau-type theories are obtained. Within the framework of this theory, we obtain a universal sequence of phases: disordered, bcc, hexagonal, lamellar, inverted hexagonal, inverted bcc, disordered, for increasing density well below the close-packing density. The sequence of phases agrees with experimental observations and with simulations of many self-assembling systems. In addition to the above phases, more complex phases may appear depending on the interaction potentials. For a particular form of the short-range attraction long-range repulsion potential, we find the bicontinuous gyroid phase ($Ia3d$ symmetry) that may be related to a network-forming cluster of colloids in a mixture of colloids and nonadsorbing polymers.

DOI: 10.1103/PhysRevE.78.061505 PACS number(s): 61.20.Gy, 61.30.St

I. INTRODUCTION

Various soft-matter systems, including surfactant solutions, globular proteins, colloids in different solvents, and colloid-polymer or star polymer–linear polymer mixtures, exhibit self-assembly into various structures. In particular, clusters or micelles of various shape and size, including branched networks, can be formed [1–9]. The clusters or micelles may exhibit ordering into different periodic phases for a range of volume fractions, including quite dilute systems. Phase separation competes in such systems with the formation of lyotropic liquid crystalline phases. Transitions between soft crystalline phases having different symmetries, phenomena such as reentrant melting [10–14], and finally formation of hard crystals are observed when the volume fraction increases. Theoretical studies of such systems can be based on liquid theories such as self-consistent Ornstein-Zernike approximation (SCOZA) [15], Landau-type theories, or density-functional theories (DFT) [16]. Unfortunately, the SCOZA cannot describe the formation of inhomogeneous microphases [17].

Landau-Ginzburg-Wilson (LGW) [18,19] theory turned out to be very successful in describing universal properties of critical phenomena associated with transitions between uniform phases. Landau-Brazovskii (LB) [20–22] theory, on the other hand, predicts universal properties of transitions between uniform and periodically ordered lyotropic liquid crystals. The statistical field-theoretic methods are very powerful in determining the effects of long-range correlations between fluctuations that lead to ordering—either to phase separation or to the formation of various ordered structures on the nanometer length scale. The effective Hamiltonians in Landau theories are given in terms of phenomenological parameters whose precise relation with thermodynamic and material properties is irrelevant for the universal, i.e., substance-independent properties. Unfortunately, the general, abstract theory has limited predicting power for particular systems.

On the other hand, in the very successful density-functional theory [16], the short-range structure is taken into account quite precisely, whereas long- and intermediate-range scale fluctuations are taken into account in a very crude mean-field approximation in most applications of the DFT. The DFT and LGW or LB theories are complementary in the treatment of the short- and long-range correlations. It is thus desirable to develop DFT with the form of the grand-thermodynamic potential functional that includes the contribution associated with the mesoscopic scale fluctuations. In order to develop such a theory, one should perform a systematic coarse-graining procedure with controllable accuracy, and derive effective Hamiltonians from the microscopic ones. Nonuniversal properties are correctly described within the collective variables (CV) [23–25] and hierarchical reference (HRT) [26,27] theories. However, the HRT is restricted to critical phenomena, and the formal structure of these theories is rather complex. Recent progress in various coarse-graining procedures is described in Refs. [28,29].

Here we propose an alternative approach, resulting in a density-functional theory with a rather simple structure. The theory allows for including in the grand potential the contribution associated with long-range correlations between fluctuations. The latter contribution can be calculated within field-theoretic methods. Within the framework of our theory, it is possible to determine phase transitions between different soft-crystalline and uniform phases. In special cases of phase separation or weak ordering into soft crystals, the theory reduces to the standard LGW or LB theories, respectively, and we obtain expressions for the coupling constants in terms of

density, temperature, and the interaction potential. Within the present approach, phase diagrams in terms of density and temperature, rather than abstract phenomenological parameters, can be obtained, and the validity of the LGW or LB theories in particular systems for given thermodynamic conditions can be verified. This kind of approach was applied already to highly charged colloids [30] and to ionic systems [31–39].

The derivation of the theory is described in Sec. II. In Sec. II A, the mesoscopic state (mesostate) is defined, and in Sec. II B, the probability distribution for the mesostates is derived from the microscopic theory. In Sec. III A, the correlation functions for the mesoscopic densities are introduced and their relation with the microscopic correlation functions is discussed. Vertex functions and the grand-potential density functional are introduced in Sec. III B. Self-consistent equations for the two-point vertex functions (related to direct correlation functions) are derived in Sec. III C. Periodic structures are considered in Sec. III D, where the approximate expression for the grand potential is also given. In Sec. IV, the general framework of the theory derived in the preceding sections is applied to a particular approximation for the probability distribution for the mesostates, related to the local-density approximation. The self-consistent equations for the two-point functions and the grand-potential functional reduce in this approximation to simpler forms given in Sec. IV B. The case of weak ordering is described in Sec. IV C, and the relation between the present theory and the Landau-type theories is discussed in Sec. IV D. Explicit results in the case of weak ordering are briefly described in Sec. V. In Sec. V A, we study the λ-line in the Brazovskii-level theory. In Sec. V B, we limit ourselves to universal features of the phase diagrams obtained in the simplest one-shell mean-field (MF) approximation, and we show the universal sequence of phases: disordered, bcc, hexagonal, lamellar, inverted hexagonal, inverted bcc, and disordered for increasing density of particles (well below the close-packing density). The details of the phase diagrams can be obtained beyond the one-shell MF approximation. However, these details depend on the shape of the interaction potential. Studies of particular systems go beyond the scope of this work and will be described elsewhere [40]. For an illustration, we consider a particular form of so called short-range attraction long-range repulsion (SALR) potential that has drawn considerable interest recently [6,17,41–48]. In Sec. V C, we quote results for a particular form of the SALR potential in the two-shell MF approximation, and we show stability of the bicontinuous gyroid phase between the hexagonal and the lamellar phases. This phase may be related to the network-forming cluster of colloids observed experimentally [6].

II. COARSE GRAINING

Let us consider spherical particles with hard cores of diameter σ that interact with arbitrary spherically symmetric potentials. A microstate is given by the sequence $\{\mathbf{r}_\alpha\}_{\alpha=1\cdots N}$ describing the positions of the centers of N spheres. The microscopic density and the energy in the microstate $\{\mathbf{r}_\alpha\}_{\alpha=1\cdots N}$ are given by

$$\hat{\rho}(\mathbf{r},\{\mathbf{r}_\alpha\}) := \sum_\alpha \delta(\mathbf{r}-\mathbf{r}_\alpha) \tag{1}$$

and

$$E[\{\mathbf{r}_\alpha\}] = \sum_{\alpha>\beta} V(|\mathbf{r}_\alpha-\mathbf{r}_\beta|), \tag{2}$$

respectively, where $V(|\mathbf{r}-\mathbf{r}'|)$ is the pair interaction potential.

A. Mesoscopic density

Let us choose the mesoscopic length scale $R \geqslant \sigma/2$ and consider spheres $S_R(\mathbf{r})$ of radius R and centers at $\mathbf{r}$ that cover the whole volume V of the system. We define the *mesoscopic* density at $\mathbf{r}$ by

$$\rho(\mathbf{r}) := \frac{1}{V_S}\int_{\mathbf{r}'\in S_R(\mathbf{r})} \hat{\rho}(\mathbf{r}',\{\mathbf{r}_\alpha\}), \tag{3}$$

where $V_S=4\pi R^3/3$. For brevity, we shall use the notation $\int_{\mathbf{r}} \equiv \int d\mathbf{r}$, indicating the integration region S by $\int_{\mathbf{r}'\in S}$ when necessary. We have $\rho(\mathbf{r})=n(\mathbf{r})/V_S$, where $n(\mathbf{r})$ is the number of the centers of hard spheres included in $S_R(\mathbf{r})$.

The set of all microstates compatible with the field $\rho(\mathbf{r})$ for given mesoscopic length scale R is called a mesostate. The microstate $\{\mathbf{r}_\alpha\}$ is compatible with the field $\rho(\mathbf{r})$, when Eq. (3) holds. In order to indicate that the microstate $\{\mathbf{r}_\alpha\}$ is compatible with the field $\rho(\mathbf{r})$ for given R, the notation $\{\mathbf{r}_\alpha\}\in\{\rho(\mathbf{r}),R\}$ will be used. For given mesoscopic length scale R, the set of all microstates can be split into disjoint subsets, such that each subset contains all microstates compatible with a particular field $\rho(\mathbf{r})$, and no other microstates.

The mesostate depends on the chosen length scale. For $R\to\infty$, the mesostate becomes identical with the macrostate. On the other hand, when $R=\sigma/2$, Eq. (3) defines the one-to-one relation between the microstates and the mesostates. The choice of R depends on the length scale λ characteristic for ordering, which is determined by the Hamiltonian. In order to describe the ordering on the length scale λ, one should choose $\sigma/2<R<\lambda/2$.

B. Probability distribution for the mesostates

Let us calculate the probability density that the mesostate $\{\rho(\mathbf{r}),R\}$ occurs in the system spontaneously. This is equal to the probability that any microstate compatible with $\rho(\mathbf{r})$ occurs. In an open system in contact with the thermostat, the probability density of the mesostate $\{\rho,R\}$ is given by

$$p[\rho] = \frac{1}{\Xi}\int_{\{\mathbf{r}_\alpha\}\in\{\rho,R\}} e^{-\beta[H-\mu\int_{\mathbf{r}}\rho(\mathbf{r})]}, \tag{4}$$

where H is the microscopic Hamiltonian and $\int_{\{\mathbf{r}_\alpha\}\in\{\rho,R\}}$ is the symbolic notation for the integration over all microstates compatible with ρ. μ and T are the chemical potential and temperature, respectively, and $\beta=1/k_BT$, with k_B denoting the Boltzmann constant. Finally,

$$\Xi = \int_{\{\mathbf{r}_\alpha\}} e^{-\beta[H-\mu\int_{\mathbf{r}}\rho(\mathbf{r})]} = \int' D\rho \int_{\{\mathbf{r}_\alpha\}\in\{\rho,R\}} e^{-\beta[H-\mu\int_{\mathbf{r}}\rho(\mathbf{r})]}. \tag{5}$$

The functional integral $\int' D\rho$ in Eq. (5) is over all mesostates $\{\rho,R\}$, which is indicated by the prime.

Fixing the mesostate in the system is equivalent to the constraint on the microstates of the form (3). In the presence of the constraint $\{\rho,R\}$, the grand potential is denoted by $\Omega_{\mathrm{co}}[\rho]$ and is given by

$$e^{-\beta\Omega_{\mathrm{co}}[\rho]} = \int_{\{\mathbf{r}_\alpha\}\in\{\rho,R\}} e^{-\beta[H-\mu\int_{\mathbf{r}}\rho(\mathbf{r})]}. \tag{6}$$

Thus, the probability density of a spontaneous occurrence of the mesostate $\{\rho,R\}$ (equal to the probability density that any of the microstates compatible with ρ occurs) is given by

$$p[\rho] = \frac{e^{-\beta\Omega_{\mathrm{co}}[\rho]}}{\Xi}, \tag{7}$$

where

$$\Xi = \int' D\rho e^{-\beta\Omega_{\mathrm{co}}[\rho]}. \tag{8}$$

We obtain a mesoscopic theory with the same structure as the standard statistical mechanics. The above formulas are exact. So far we just rearranged the summation over microstates. In Eq. (8), the integration over microstates compatible with each mesostate is included in Ω_{co}, and then we perform a summation over all mesostates. The reason for doing so is the possibility of performing the summation over the mesostates and over the microstates compatible with a particular mesostate within the field-theoretic and density-functional methods, respectively. With this form of coarse-graining, one can consider the system of particles in terms of fields, and obtain results in terms of interaction potential and thermodynamic variables. In a similar way, one can define a mesoscopic theory for the mesoscopic volume fraction.

Note that in the mesoscopic theory, the mesostate $\{\rho_0,R\}$ that corresponds to the global minimum of $\Omega_{\mathrm{co}}[\rho]$ is analogous to the ground state in the microscopic theory. The ground state corresponds to *the most probable single microstate*. Likewise $\{\rho_0,R\}$ is *the single mesostate that occurs with the highest probability*.

III. GRAND POTENTIAL AND THE CORRELATION FUNCTIONS FOR THE MESOSCOPIC DENSITIES

The grand potential in the system subject to the constraint for the mesoscopic density distribution $\rho(\mathbf{r})$ can be written in the form

$$\Omega_{\mathrm{co}} = U - TS - \mu N, \tag{9}$$

where U,S,N are the internal energy, entropy, and the number of molecules, respectively, in the system with the constraint (3) imposed on the microscopic densities. U is given by the well known expression

$$U[\rho^*] = \frac{1}{2}\int_{\mathbf{r}_1}\int_{\mathbf{r}_2} V_{\mathrm{co}}(\mathbf{r}_1-\mathbf{r}_2)\rho^*(\mathbf{r}_1)\rho^*(\mathbf{r}_2), \tag{10}$$

where

$$V_{\mathrm{co}}(\mathbf{r}_1-\mathbf{r}_2) = V(r_{12})g_{\mathrm{co}}(\mathbf{r}_1-\mathbf{r}_2), \tag{11}$$

$r_{12}=|\mathbf{r}_1-\mathbf{r}_2|$, and $g_{\mathrm{co}}(\mathbf{r}_1-\mathbf{r}_2)$ is the microscopic pair correlation function in the system with the constraint (3) imposed on the microscopic states. From now on we consider dimensionless density

$$\rho^* = \rho\sigma^3. \tag{12}$$

In the case of the considered systems (no internal degrees of freedom of the particles), the entropy S satisfies the relation $-TS=F_h$, where F_h is the free energy of the reference hard-sphere system with the constraint (3) imposed on the microscopic densities.

A. Correlation functions for the mesoscopic densities and their generating functional

Let us introduce an external field $J(\mathbf{r})$ and the grand-thermodynamic potential functional

$$\Omega[\beta J] := -k_BT\ln\left[\int' D\rho^* e^{-\beta\{\Omega_{\mathrm{co}}[\rho^*]-\int_{\mathbf{r}}J(\mathbf{r})\rho^*(\mathbf{r})\}}\right]. \tag{13}$$

The generating functional for the (connected) correlation functions for the mesoscopic densities is $-\beta\Omega[\beta J]$, and

$$\langle\rho^*(\mathbf{r}_1)\cdots\rho^*(\mathbf{r}_n)\rangle^{\mathrm{con}} = \frac{\delta^n(-\beta\Omega[\beta J])}{\delta(\beta J(\mathbf{r}_1))\cdots\delta(\beta J(\mathbf{r}_n))}. \tag{14}$$

In particular, the above gives

$$\langle\rho^*(\mathbf{r})\rangle = \frac{\int' D\rho^* e^{-\beta[\Omega_{\mathrm{co}}[\rho^*]-\int_{\mathbf{r}}J(\mathbf{r})\rho^*(\mathbf{r})]}\rho^*(\mathbf{r})}{\int' D\rho e^{-\beta[\Omega_{\mathrm{co}}[\rho^*]-\int_{\mathbf{r}}J(\mathbf{r})\rho^*(\mathbf{r})]}} = \frac{\sigma^3}{V_S}\int_{\mathbf{r}'\in S(\mathbf{r})}\langle\hat{\rho}(\mathbf{r}')\rangle, \tag{15}$$

where Eqs. (3), (6), and (5) were used. We use the same notation $\langle\cdots\rangle$ for the microscopic and the mesoscopic average. The average value of the *mesoscopic* density at the point $\mathbf{r}$ is the average *microscopic* density *integrated* over the sphere $S_R(\mathbf{r})$ of the radius R, and divided by its volume V_S. Clearly, $\langle\rho^*(\mathbf{r})\rangle$ depends on R. If, however, $\langle\rho^*(\mathbf{r})\rangle$ is independent of R for some range of $\sigma/2<R<\lambda/2$, then this function gives information about actual ordering on the length scale λ.

For the correlation function for the mesoscopic density, we introduce the notation

$$\mathcal{G}_2(\mathbf{r}_1,\mathbf{r}_2) = \langle\rho^*(\mathbf{r}_1)\rho^*(\mathbf{r}_2)\rangle^{\mathrm{con}}, \tag{16}$$

where here and below the superscript "con" denotes

$$\langle A(\rho^*(\mathbf{r}_1))B(\rho^*(\mathbf{r}_2))\rangle^{\mathrm{con}} = \langle A(\rho^*(\mathbf{r}_1))B(\rho^*(\mathbf{r}_2))\rangle - \langle A(\rho^*(\mathbf{r}_1))\rangle\langle B(\rho^*(\mathbf{r}_2))\rangle, \tag{17}$$

and where

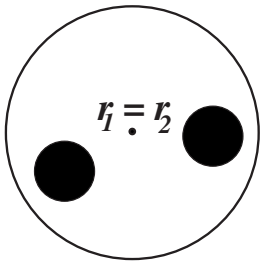

FIG. 1. Microscopic configuration contributing to the correlation function $\mathcal{G}_2(\mathbf{r}_1,\mathbf{r}_2)$ for $\mathbf{r}_1=\mathbf{r}_2$ in the case of $R>\sigma/2$. The black circles represent particles, and the open circle represents the coinciding spheres $S_R(\mathbf{r}_1)=S_R(\mathbf{r}_2)$, over which the microscopic correlations are averaged. Note that the black spheres do not overlap, and their centers are both included in S_R. Thus, the microscopic correlation function for this microstate does not vanish.

$$\langle \rho^*(\mathbf{r}_1)\rho^*(\mathbf{r}_2)\rangle = \frac{\int' D\rho e^{-\beta\{\Omega_{\rm co}[\rho^*]-\int_{\mathbf{r}}J(\mathbf{r})\rho^*(\mathbf{r})\}}\rho^*(\mathbf{r}_1)\rho^*(\mathbf{r}_2)}{\int' D\rho e^{-\beta\{\Omega_{\rm co}[\rho^*]-\int_{\mathbf{r}}J(\mathbf{r})\rho^*(\mathbf{r})\}}} = \frac{\sigma^3}{V_S}\int_{\mathbf{r}'\in S(\mathbf{r}_1)}\frac{\sigma^3}{V_S}\int_{\mathbf{r}''\in S(\mathbf{r}_2)}\langle\hat{\rho}(\mathbf{r}')\hat{\rho}(\mathbf{r}'')\rangle. \tag{18}$$

The correlation function for the *mesoscopic* density at $\mathbf{r}_1$ and $\mathbf{r}_2$ is the correlation function for the *microscopic* density at the points $\mathbf{r}'\in S_R(\mathbf{r}_1)$ and $\mathbf{r}''\in S_R(\mathbf{r}_2)$, *integrated over the spheres* $S_R(\mathbf{r}_1)$ and $S_R(\mathbf{r}_2)$, respectively. While the *microscopic* pair distribution function vanishes for $|\mathbf{r}'-\mathbf{r}''|<\sigma$, the *mesoscopic* quantity defined by Eqs. (16)–(18) does not vanish for $\mathbf{r}_1=\mathbf{r}_2$ (see Fig. 1).

B. Grand-potential functional of the mesoscopic density, and the vertex functions

Let us introduce the Legendre transform

$$\beta F[\bar{\rho}^*] := \beta\Omega[\beta J] + \int_{\mathbf{r}}\beta J(\mathbf{r})\bar{\rho}^*(\mathbf{r}), \tag{19}$$

where

$$\bar{\rho}^*(\mathbf{r}) = \frac{\delta(-\beta\Omega)}{\delta(\beta J(\mathbf{r}))} \tag{20}$$

is the dimensionless average field for given $J(\mathbf{r})$. The equation of state takes the form

$$\frac{\delta(\beta F)}{\delta\bar{\rho}^*(\mathbf{r})} = \beta J(\mathbf{r}). \tag{21}$$

In general, $\bar{\rho}^*$ may differ from any mesostate defined by Eq. (3). Let the extension of the functional $\Omega_{\rm co}$ be defined in Eq. (9) on the Hilbert space of fields f, such that in Fourier representation $\tilde{f}(\mathbf{k})=0$ for the wave numbers $k\geqslant\pi/R$. Here and below $\tilde{f}(\mathbf{k})$ is the Fourier transform of $f(\mathbf{r})$. There is no restriction on the magnitude of the fields $\tilde{f}(\mathbf{k})$ that belong to the Hilbert space. On the other hand, the mesoscopic density is bounded from above by the close-packing density. However, the fields $\tilde{\rho}^*(\mathbf{k})$ with large values yield large values of $\Omega_{\rm co}$ [see Eqs. (9) and (10)], and in turn small values of the Boltzmann factor (7), therefore inclusion of such fields in the Hilbert space should not have a large effect on the results. Self-consistency of the approach requires that the average density obtained within this theory is bounded from above by the close-packing density.

We can define

$$H_{\rm fluc}[\bar{\rho}^*,\phi] = \Omega_{\rm co}[\bar{\rho}^*+\phi]-\Omega_{\rm co}[\bar{\rho}^*] = \sum_{n=1}\int_{\mathbf{r}_1}\cdots\int_{\mathbf{r}_n}\frac{\mathcal{C}_n^{\rm co}(\mathbf{r}_1,\ldots,\mathbf{r}_n|\bar{\rho}^*]}{n!}\phi(\mathbf{r}_1)\cdots\phi(\mathbf{r}_n), \tag{22}$$

where $\bar{\rho}^*$ is given in Eq. (20) and $\mathcal{C}_n^{\rm co}(\mathbf{r}_1,\ldots,\mathbf{r}_n|\bar{\rho}^*]$ is the nth functional derivative of $\Omega_{\rm co}[\rho^*]$ at $\rho^*=\bar{\rho}^*$. By definition, $\langle\phi\rangle=0$. Then from Eqs. (13) and (19), we obtain

$$-\beta\Omega[\beta J] = -\beta\Omega_{\rm co}[\bar{\rho}^*] + \int_{\mathbf{r}}\beta J(\mathbf{r})\bar{\rho}^*(\mathbf{r}) + \ln\left[\int D\phi e^{-\beta[H_{\rm fluc}-\int_{\mathbf{r}}J(\mathbf{r})\phi(\mathbf{r})]}\right] \tag{23}$$

and

$$\beta F[\bar{\rho}^*] = \beta\Omega_{\rm co}[\bar{\rho}^*] - \ln\left[\int D\phi e^{-\beta[H_{\rm fluc}-\int_{\mathbf{r}}J(\mathbf{r})\phi(\mathbf{r})]}\right]. \tag{24}$$

Equation (24) defines the functional in which the microscopic scale fluctuations, with frozen fluctuations of the mesoscopic density over the length scales larger than R, are included in the first term, and the mesoscopic scale fluctuations are included in the last term. Equation (24) should serve as a starting point for various approximate theories. The idea is to apply approximate microscopic theories to the first term, and field-theoretic approaches to the second term.

C. Equations for the correlation functions

Note that from Eq. (24) it follows that the vertex functions (related to the direct correlation functions) defined by

$$\mathcal{C}_n(\mathbf{r}_1,\ldots,\mathbf{r}_n) = \frac{\delta^n\beta F[\bar{\rho}^*]}{\delta\bar{\rho}^*(\mathbf{r}_1)\cdots\delta\bar{\rho}^*(\mathbf{r}_n)} \tag{25}$$

consist of two terms: the first one is the contribution from the fluctuations on the microscopic length scale ($<R$) with frozen fluctuations on the mesoscopic length scale, the second one is the contribution from the fluctuations on the mesoscopic length scale ($>R$).

The average density for $J=0$ satisfies the equation [see Eqs. (21) and (24)]

$$\frac{\delta\beta\Omega_{\rm co}[\bar{\rho}^*]}{\delta\bar{\rho}^*(\mathbf{r})} + \left\langle\frac{\delta(\beta H_{\rm fluc})}{\delta\bar{\rho}^*(\mathbf{r})}\right\rangle = 0, \tag{26}$$

where the averaging is over the fields ϕ with the probability $\propto\exp(-\beta H_{\rm fluc}[\bar{\rho}^*,\phi])$. For the two-point function from Eqs. (25) and (24), we obtain the equation

$$2\mathcal{C}_2(\mathbf{r}_1,\mathbf{r}_2) = \mathcal{C}_2^{\rm co}(\mathbf{r}_1,\mathbf{r}_2) + \left\langle \frac{\delta^2(\beta H_{\rm fluc})}{\delta\bar{\rho}^*(\mathbf{r}_1)\delta\bar{\rho}^*(\mathbf{r}_2)} \right\rangle - \left\langle \frac{\delta(\beta H_{\rm fluc})}{\delta\bar{\rho}^*(\mathbf{r}_1)} \frac{\delta(\beta H_{\rm fluc})}{\delta\bar{\rho}^*(\mathbf{r}_2)} \right\rangle^{\rm con} + \int_{\mathbf{r}'} \left[\left\langle \frac{\delta H_{\rm fluc}}{\delta\bar{\rho}^*(\mathbf{r}_1)} \phi(\mathbf{r}') \right\rangle \mathcal{C}_2(\mathbf{r}',\mathbf{r}_2) + \left\langle \frac{\delta H_{\rm fluc}}{\delta\bar{\rho}^*(\mathbf{r}_2)} \phi(\mathbf{r}') \right\rangle \mathcal{C}_2(\mathbf{r}',\mathbf{r}_1) \right]. \quad (27)$$

In calculating the functional derivative of F [Eq. (24)], we used the equality $\delta J(\mathbf{r}_1)/\delta\bar{\rho}^*(\mathbf{r}_2) = \mathcal{C}_2(\mathbf{r}_1,\mathbf{r}_2)$ [see Eq. (21)]. From Eq. (22), we have

$$\frac{\delta^m(\beta H_{\rm fluc})}{\delta\bar{\rho}^*(\mathbf{r})\cdots\delta\bar{\rho}^*(\mathbf{r}^{(m)})} = \sum_{n=1}^{\infty} \int_{\mathbf{r}_1} \cdots \int_{\mathbf{r}_n} \frac{\mathcal{C}_{n+m}^{\rm co}(\mathbf{r}_1,\ldots,\mathbf{r}_n,\mathbf{r},\ldots,\mathbf{r}^{(m)}|\bar{\rho}^*)}{n!} \times \phi(\mathbf{r}_1)\cdots\phi(\mathbf{r}_n). \quad (28)$$

Higher-order vertex functions can be obtained from Eqs. (25) and (24) in a similar way. As a result, a hierarchy of equations where the vertex functions are expressed in terms of the many-body correlation functions is obtained.

In the mean-field approximation, the fluctuation contribution is just neglected. In the lowest-order nontrivial approximation, the expansion in Eq. (28) is truncated at $n=2$, and only terms proportional to the pair-correlation function $\langle\phi(\mathbf{r})\phi(\mathbf{r}')\rangle$ are included in Eqs. (26) and (27). Then Eqs. (26) and (27) assume the approximate forms

$$\frac{\delta\beta\Omega_{\rm co}[\bar{\rho}^*]}{\delta\bar{\rho}^*(\mathbf{r})} + \int_{\mathbf{r}_1}\int_{\mathbf{r}_2} \mathcal{G}_2(\mathbf{r}_1,\mathbf{r}_2)\mathcal{C}_3^{\rm co}(\mathbf{r}_1,\mathbf{r}_2,\mathbf{r}) = 0 \quad (29)$$

and

$$2\mathcal{C}_2(\mathbf{r}_1,\mathbf{r}_2) = 3\mathcal{C}_2^{\rm co}(\mathbf{r}_1,\mathbf{r}_2) + \int_{\mathbf{r}}\int_{\mathbf{r}'} \mathcal{G}_2(\mathbf{r},\mathbf{r}') \left[\frac{\mathcal{C}_4^{\rm co}(\mathbf{r},\mathbf{r}',\mathbf{r}_1,\mathbf{r}_2)}{2} - \mathcal{C}_2^{\rm co}(\mathbf{r},\mathbf{r}_1)\mathcal{C}_2^{\rm co}(\mathbf{r}',\mathbf{r}_2) \right]. \quad (30)$$

From Eqs. (21) and (14), we obtain the analog of the Ornstein-Zernicke equation,

$$\int_{\mathbf{r}_2} \mathcal{C}_2(\mathbf{r}_1,\mathbf{r}_2)\mathcal{G}_2(\mathbf{r}_2,\mathbf{r}_3) = \delta(\mathbf{r}_1-\mathbf{r}_3). \quad (31)$$

We assume that the form of $\Omega_{\rm co}$ is known from the microscopic theory. Self-consistent solutions of Eqs. (30) and (31) yield the two-point vertex and correlation functions, $\mathcal{C}_2$ and $\mathcal{G}_2$, respectively, for given forms of $\mathcal{C}_n^{\rm co}$. Note that Eq. (30) plays a role of the closure to the OZ equation (31). Equation (29) is the minimum condition for the grand potential, and corresponds to a stable or to a metastable phase. The solution of Eq. (29) corresponding to the global minimum gives the average density for given μ and T in the lowest nontrivial order beyond MF.

In the rest of this work, we limit ourselves to the approximate theory based on the two-point correlation functions.

D. Periodic structures; general case

Let us consider periodic density profiles

$$\bar{\rho}^*(\mathbf{r}) = \bar{\rho}_0^* + \Phi(\mathbf{r}), \quad (32)$$

where

$$\Phi(\mathbf{r}+\mathbf{P}) = \Phi(\mathbf{r}) \quad (33)$$

and $\mathbf{P}=\Sigma_i^3 n_i\mathbf{p}_i$, where $\mathbf{p}_i$ are the vectors connecting the centers of the nearest-neighbor unit cells and n_i are integer. The $\bar{\rho}_0^*$ is the space-averaged density, i.e.,

$$\int_{\mathbf{r}\in\mathcal{V}_u} \Phi(\mathbf{r}) = 0, \quad (34)$$

where $\mathcal{V}_u$ is the unit cell of the periodic structure, whose volume is denoted by V_u. In the case of periodic structures,

$$\mathcal{C}_2(\mathbf{r}_1+\mathbf{P},\mathbf{r}_2+\mathbf{P}) = \mathcal{C}_2(\mathbf{r}_1,\mathbf{r}_2) = \mathcal{C}_2(\Delta\mathbf{r}|\mathbf{r}_2), \quad (35)$$

where $\Delta\mathbf{r}=\mathbf{r}_1-\mathbf{r}_2\in R^3$ and $\mathbf{r}_2\in\mathcal{V}_u$.

Let us consider the Gaussian functional

$$\mathcal{H}_G[\bar{\rho}^*,\phi] := \frac{1}{2}\int_{\mathbf{r}_1}\int_{\mathbf{r}_2} \phi(\mathbf{r}_1)\mathcal{C}_2(\mathbf{r}_1-\mathbf{r}_2|\mathbf{r}_2)\phi(\mathbf{r}_2) = \frac{1}{2}\int_{\mathbf{k}}\int_{\mathbf{k}'} \tilde{\phi}(\mathbf{k})\tilde{\mathcal{C}}_2(\mathbf{k},\mathbf{k}+\mathbf{k}')\tilde{\phi}(\mathbf{k}'). \quad (36)$$

Here and below we use the simplified notation $\int_{\mathbf{k}} = \int d\mathbf{k}/(2\pi)^3$. For periodic structures, we have (see Appendix A)

$$\mathcal{H}_G[\bar{\rho}^*,\phi] = \frac{1}{2}\int_{\mathbf{k}} \tilde{\phi}(\mathbf{k})\tilde{C}_2(\mathbf{k})\tilde{\phi}(-\mathbf{k}), \quad (37)$$

where $\tilde{C}_2(\mathbf{k})$ is the Fourier transform of the vertex function averaged over the unit cell,

$$C_2(\Delta\mathbf{r}) := \frac{1}{V_u}\int_{\mathbf{r}_2\in\mathcal{V}_u} \mathcal{C}_2(\Delta\mathbf{r}|\mathbf{r}_2). \quad (38)$$

From the analog of the Ornstein-Zernicke equation (31), we obtain the relation

$$\tilde{C}_2(\mathbf{k})\tilde{G}_2(\mathbf{k}) = 1, \quad (39)$$

where

$$\tilde{G}_2(\mathbf{k}) = \int_{\mathbf{r}_1-\mathbf{r}_2} e^{i\mathbf{k}\cdot(\mathbf{r}_1-r_2)} \frac{1}{V_u}\int_{\mathbf{r}_1\in\mathcal{V}_u} \mathcal{G}_2(\mathbf{r}_1,\mathbf{r}_2) = \int_{\mathbf{r}_1-\mathbf{r}_2} e^{i\mathbf{k}\cdot(\mathbf{r}_1-\mathbf{r}_2)} G_2(\mathbf{r}_1-\mathbf{r}_2). \quad (40)$$

In order to calculate the second term in Eq. (24), we follow the standard field-theoretic procedure and write

$$H_{\mathrm{fluc}}[\bar{\rho}^*,\phi] = \mathcal{H}_G[\bar{\rho}^*,\phi] + \Delta\mathcal{H}[\bar{\rho}^*,\phi], \tag{41}$$

where $\mathcal{H}_G[\bar{\rho}^*,\phi]$ is the Gaussian functional (37). Next we make an assumption that $\Delta H[\bar{\rho}^*,\phi]$ can be treated as a small perturbation. When such an assumption is valid, we obtain [22,36]

$$\beta\Omega[\bar{\rho}^*] \approx \beta\Omega_{\mathrm{co}}[\bar{\rho}^*] - \ln \int D\phi e^{-\beta\mathcal{H}_G} + \langle\beta\Delta\mathcal{H}\rangle_G + O(\langle\beta\Delta\mathcal{H}\rangle_G^2), \tag{42}$$

where $\langle\cdots\rangle_G$ denotes averaging with the Gaussian Boltzmann factor $\propto e^{-\beta\mathcal{H}_G}$. In general, each contribution to Eq. (42) depends on the mesoscopic length scale R, but the R-dependent contributions must cancel against each other to yield R-independent Ω.

IV. APPROXIMATE THEORY: LOCAL-DENSITY APPROXIMATION FOR Ω_{co}

In our theory, different levels of approximation for Ω_{co} are possible. For an illustration, we demonstrate the mesoscopic theory with the microscopic degrees of freedom considered in a very crude approximation. In this approximation, calculations are greatly simplified and analytical methods can be used. However, the validity of the approximate theory is limited to low or moderate densities. Next we show how the functional can be further simplified to the Landau-type form, and discuss in what cases such a reduction is justified. The expressions for the phenomenological parameters in the Landau-type theory are given in terms of the thermodynamic variables and V_{co}.

A. Derivation of the functional Ω_{co} in the local-density approximation

In order to derive an approximate form of Ω_{co} [Eq. (9)], we need an approximate form of the microscopic pair correlation function. The microscopic correlation function has the limiting behavior

$$g_{\mathrm{co}}(\mathbf{r}_1-\mathbf{r}_2) = 0 \quad \text{for} \quad |\mathbf{r}_1-\mathbf{r}_2| < \sigma,$$

$$g_{\mathrm{co}}(\mathbf{r}_1-\mathbf{r}_2) \to 1 \quad \text{for} \quad |\mathbf{r}_1-\mathbf{r}_2| \to \infty. \tag{43}$$

If the ordering in the system occurs on the length scale λ larger than $R \gg \sigma/2$, then the precise form of g_{co} is not crucial and in the simplest approximation we assume

$$g_{\mathrm{co}}(\mathbf{r}_1-\mathbf{r}_2) = \theta(|\mathbf{r}_1-\mathbf{r}_2|-\sigma). \tag{44}$$

In order to develop an approximation for the entropy S in the presence of the constraint imposed on the density profile, let us consider the number of the microstates associated with different positions of the centers of particles included in the sphere $S_R(\mathbf{r})$ for given $\rho(\mathbf{r})$. We assume that the corresponding contribution to the entropy depends only weakly on the mesoscopic density at $\mathbf{r}'$ when $|\mathbf{r}-\mathbf{r}'| \gg R$. When this assumption is satisfied, then the local-density approximation can be applied, and

$$F_h[\rho^*] = \int_{\mathbf{r}} f_h(\rho^*(\mathbf{r})), \tag{45}$$

where $f_h(\rho^*)$ is the free-energy density of the hard-sphere system of density $\rho^*=\rho\sigma^3$. For the latter we may assume the Percus-Yevick (PY) or the Carnahan-Starling approximation. We choose the former case (compressibility route) and assume

$$\beta f_h(\rho^*) = \rho^*\ln(\rho^*) - \rho^* + \rho^*\left[\frac{3\eta(2-\eta)}{2(1-\eta)^2} - \ln(1-\eta)\right], \tag{46}$$

where $\eta=\pi\rho^*/6$. In this simple approximation, we obtain the R-independent functional

$$\beta\Omega_{\mathrm{co}}[\rho^*] = \frac{1}{2}\int_{\mathbf{r}_1}\int_{\mathbf{r}_2}\beta V_{\mathrm{co}}(r_{12})\rho^*(\mathbf{r}_1)\rho^*(\mathbf{r}_2) - \int_{\mathbf{r}}\beta f_h(\rho^*(\mathbf{r})) - \int_{\mathbf{r}}\beta\mu\rho^*(\mathbf{r}), \tag{47}$$

where $V_{\mathrm{co}}(r_{12})$ is defined in Eq. (11), and for $g_{\mathrm{co}}(r_{12})$ we make the assumption (44).

For $F_h[\rho^*]$ given by Eq. (45), i.e., for the local-density approximation, the functional derivatives of the functional Ω_{co} take the forms

$$\mathcal{C}_n^{\mathrm{co}}(\mathbf{r}_1,\ldots,\mathbf{r}_n|\bar{\rho}^*] = \begin{cases} \delta(\mathbf{r}_1-\mathbf{r}_2)\cdots\delta(\mathbf{r}_{n-1}-\mathbf{r}_n)\beta f_h^{(n)}(\bar{\rho}^*(\mathbf{r}_1)) & \text{for } n\geqslant 3 \\ \beta(f_h^{(2)}(\bar{\rho}^*(\mathbf{r}_1))\delta(\mathbf{r}_1-\mathbf{r}_2) + V_{\mathrm{co}}(r_{12})) & \text{for } n=2 \\ \beta\left(f_h^{(1)}(\bar{\rho}^*(\mathbf{r}_1)) - \mu + \int_{\mathbf{r}_2} V_{\mathrm{co}}(r_{12})\bar{\rho}^*(\mathbf{r}_2)\right) & \text{for } n=1, \end{cases} \tag{48}$$

where $f_h^{(n)}(\bar{\rho}^*(\mathbf{r}))$ denotes the nth derivative of f_h with respect to its argument, calculated at $\rho^*(\mathbf{r})=\bar{\rho}^*(\mathbf{r})$. In the local-density approximation, Eq. (22) assumes the simpler form

$$\beta H_{\mathrm{fluc}}[\bar{\rho}^*,\phi] = \beta\Omega_{\mathrm{co}}[\bar{\rho}^*+\phi] - \beta\Omega_{\mathrm{co}}[\bar{\rho}^*] = \frac{1}{2}\int_{\mathbf{r}_1}\int_{\mathbf{r}_2}\phi(\mathbf{r}_1)\mathcal{C}_2^{\mathrm{co}}(\mathbf{r}_1,\mathbf{r}_2)\phi(\mathbf{r}_2) + \int_{\mathbf{r}}\mathcal{C}_1^{\mathrm{co}}(\mathbf{r})\phi(\mathbf{r}) + \sum_{n=3}\int_{\mathbf{r}}\frac{\beta f_h^{(n)}(\bar{\rho}^*(\mathbf{r}))}{n!}\phi(\mathbf{r})^n. \tag{49}$$

The dominant contribution to the second term in Eq. (24) comes from small fields ϕ. For fields with small values, the expansion in Eq. (49) can be truncated. For stability reasons, the ϕ^4 term must be included.

B. Periodic structures in the local-density approximation

Let us consider the grand-potential functional (42) in the local-density approximation, i.e., with $\Omega_{\rm co}$ given in Eq. (47), and let us focus on the fluctuation contribution. From the results of Sec. III D, and Eqs. (30), (39), (40), and (48), we obtain the equation for $\tilde{C}_2(k)$,

$$2\tilde{C}_2(k) = 3\tilde{C}_2^{\rm co}(k) + \frac{\beta \bar{f}_h^{(4)}[\bar{\rho}^*]}{2}\mathcal{G} - \frac{\tilde{C}_2^{\rm co}(k)^2}{\tilde{C}_2(k)}, \tag{50}$$

where

$$\tilde{C}_2^{\rm co}(k) = \beta[\tilde{V}_{\rm co}(k) + \bar{f}_h^{(2)}[\bar{\rho}^*]], \tag{51}$$

and we introduced the notation

$$\bar{f}_h^{(n)}[\bar{\rho}^*] = \frac{1}{V_u}\int_{\mathbf{r}\in\mathcal{V}_u} f_h^{(n)}(\bar{\rho}_0^*(\mathbf{r})) \tag{52}$$

and

$$\mathcal{G} = \int_{\mathbf{k}} \frac{1}{\tilde{C}_2(k)} = \int_{\mathbf{k}} \tilde{G}_2(k). \tag{53}$$

Recall that by construction of the mesoscopic theory on the length scale R, the cutoff $\sim\pi/R$ is present in the above integral.

In this approximation, the grand-thermodynamic potential (42) takes the explicit form

$$\beta\Omega[\bar{\rho}^*]/V \approx \beta\Omega_{\rm co}[\bar{\rho}^*]/V + \frac{1}{2}\int_{\mathbf{k}} \ln\left(\frac{\tilde{C}_2(k)}{2\pi}\right) + \frac{1}{2}\int_{\mathbf{k}}\left[\frac{\tilde{C}_2^{\rm co}(k)}{\tilde{C}_2(k)} - 1\right] + \frac{\bar{f}_4[\bar{\rho}^*]\mathcal{G}^2}{8}, \tag{54}$$

with $\Omega_{\rm co}$ and $\tilde{C}_2^{\rm co}(k)$ given in Eqs. (47) and (51), respectively, and $\tilde{C}_2(k)$ determined from Eqs. (50)–(53). The second term on the right-hand side (RHS) in Eq. (54) is the explicit form of the second term on the RHS in Eq. (42). In calculating the third term on the RHS in Eq. (42), the property $\langle\phi(\mathbf{r})^{2n+1}\rangle_G = 0$ was used.

The presence of the fluctuation contribution distinguishes this expression from standard forms of $\Omega[\bar{\rho}^*]$ in density-functional theories. On the other hand, the form of the first term is much more accurate than in the phenomenological Landau-type theories. Moreover, the fluctuation contribution and the equation for the correlation function differ from their counterparts in the phenomenological Landau-type theories. In particular, they are given in terms of the interaction potential, thermodynamic parameters, and quantities (52), rather than phenomenological parameters.

C. Case of weak ordering

Let us consider the functional (49) for the periodic density profiles (32) in the case of weak ordering, i.e., when $\Phi \ll \bar{\rho}_0^*$. When the expansion in ϕ is truncated at the fourth-order term, then in the consistent approximation, the Taylor expansion

$$f_h^{(n)}(\bar{\rho}^*(\mathbf{r})) = f_h^{(n)}(\bar{\rho}_0^*) + \sum_{m=1}^{\infty} \frac{f_h^{(n+m)}(\bar{\rho}_0^*)}{m!}\Phi(\mathbf{r})^m \tag{55}$$

is truncated at the fourth-order term in Φ. In this approximation, Eq. (49) assumes for periodic density profiles (32) the form

$$\beta H_{\rm fluc}[\Phi,\phi] = \frac{1}{2}\int_{\mathbf{k}} \tilde{\phi}(\mathbf{k})\tilde{C}_2^{\rm co}(k,\Phi)\tilde{\phi}(-\mathbf{k}) + \int_{\mathbf{r}} {\sum_{n\geqslant 1}}' \frac{C_n^{\rm co}[\bar{\rho}_0^*,\Phi,\mathbf{r}]}{n!}\phi(\mathbf{r})^n, \tag{56}$$

where the prime in the above sum means that $n \neq 2$, the explicit expressions for $C_n^{\rm co}$ are given in Appendix B, and the function $\tilde{C}_2^{\rm co}(k,\Phi)$ has the explicit form

$$\tilde{C}_2^{\rm co}(k,\Phi) = \tilde{C}_2^0(k) + \frac{\beta f_h^{(4)}(\bar{\rho}_0^*)}{2}\Phi^2 \tag{57}$$

with

$$\tilde{C}_2^0(k) = \beta[\tilde{V}_{\rm co}(k) + f_h^{(2)}(\bar{\rho}_0^*)] \tag{58}$$

and

$$\Phi^2 = \frac{1}{V_u}\int_{\mathbf{r}\in\mathcal{V}_u} \Phi(\mathbf{r})^2. \tag{59}$$

In this approximation, $\tilde{C}_2(k)$ is given in Eq. (50) with $\bar{f}_h^{(4)}[\bar{\rho}^*]$ approximated by $f_h^{(4)}(\bar{\rho}_0^*)$, and $\beta\Omega_{\rm co}[\bar{\rho}^*]$ [Eq. (47)] can be approximated by

$$\beta\Omega_{\rm co}[\bar{\rho}_0^* + \Phi] = \beta\Omega_{\rm co}[\bar{\rho}_0^*] + \frac{1}{2}\int_{\mathbf{k}} \tilde{\Phi}(\mathbf{k})\tilde{C}_2^0(k)\tilde{\Phi}(-\mathbf{k}) + \sum_{n\geqslant 3}\frac{f_h^{(n)}(\bar{\rho}_0^*)}{n!}\int_{\mathbf{r}}\Phi(\mathbf{r})^n. \tag{60}$$

D. Comparison with the Landau-type theory

After all the assumptions and approximations described above, namely (i) $\lambda \gg \sigma$ (this allows for the local-density approximation for $\Omega_{\rm co}$), (ii) periodically ordered structures, and (iii) weak ordering ($\Phi \ll \bar{\rho}_0^*$), we finally arrived at the form of $\Omega_{\rm co}$, Eq. (60), and $H_{\rm fluc}$, Eq. (56), similar to the Landau-Ginzburg-Wilson and Landau-Brazovskii theories. In the original Landau-Ginzburg-Wilson and Landau-Brazovskii theories focusing on universal features of the order-disorder transition, it is *postulated* that the effective or coarse-grained Hamiltonian in the uniform system has the form

$$\beta H_{\text{eff}}[\phi] = \frac{1}{2}\int_{\mathbf{k}} \tilde{\phi}(\mathbf{k})\tilde{C}_2^0(k)\tilde{\phi}(-\mathbf{k}) + \int_{\mathbf{r}} \left[h\phi(\mathbf{r}) + \sum_{n=3}^{4} \frac{A_n}{n!}\phi^n(\mathbf{r}) \right]. \quad (61)$$

The summation in Eq. (61) is truncated at $n=6$ when a tricritical point is studied. The form of $\tilde{C}_2^0(k)$ is

$$\tilde{C}_2^0(k) = \tau_0 + \xi_0^2 k^2 \quad (62)$$

or

$$\tilde{C}_2^0(k) = \tau_0 + \xi_0^2 (k - k_b)^2 \quad (63)$$

in the LGW and LB theories, respectively. In the original Brazovskii theory, only even powers of the field are included ($h=A_3=0$). [In some variants of the LB theory, $\tilde{C}_2^0(k)=\tau_0+\bar{\xi}_0^2(k^2-k_b^2)^2$; for $k\approx k_b$, the latter reduces to Eq. (63) with $\xi_0=2k_b\bar{\xi}_0$.] In nonuniform systems, with the equilibrium density profile $\bar{\rho}^*(\mathbf{r})$, one obtains the effective Hamiltonian $H_{\text{eff}}[\bar{\rho}^*(\mathbf{r})+\phi(\mathbf{r})]$ as a functional of the fluctuation $\phi(\mathbf{r})$.

Note that in the case of the uniform phase ($\Phi=0$), Eq. (56) can be reduced to the LGW or LB functional (61) with the following expressions for the coupling constants:

$$A_n = \beta f_h^{(n)}(\bar{\rho}_0^*) \quad (64)$$

for $n \geqslant 3$ and

$$h = \beta(f_h^{(1)}(\bar{\rho}_0^*) - \mu - \tilde{V}_{\text{co}}(0)\bar{\rho}_0^*). \quad (65)$$

The explicit forms of $f_h^{(n)}(\bar{\rho}_0^*)$ are given in Appendix C for f_h approximated by Eq. (46). However, in our theory $\tilde{C}_2^0(k)$ is given in Eq. (58).

When $\tilde{V}_{\text{co}}(k)$ assumes the global minimum for $k=k_b=0$, and can be expanded about $k=0$, then Eq. (62) corresponds to this expansion truncated at the second-order term. Truncation of the expansion of $\tilde{V}_{\text{co}}(k)$ is justified when the fields $\tilde{\rho}^*(\mathbf{k})$ with large k yield negligible contribution to Ω. This is the case in which thermally excited density waves with large k are associated with significantly larger energy than the density waves with the wave number $k\to 0$, and can be disregarded. The above conditions are satisfied when the global minimum is deep, and local minima, if they exist, correspond to significantly larger values of $\tilde{V}_{\text{co}}(k)$. More precisely, the interaction potential should satisfy the condition $|\tilde{V}_{\text{co}}(k) - [\tilde{V}_{\text{co}}(0)+\tilde{V}_{\text{co}}^{(2)}(0)k^2]|/|\tilde{V}_{\text{co}}(k)| \ll 1$ for k that yields the dominant contribution to Ω. Under the above conditions, our mesoscopic theory reduces to the Landau-Ginzburg-Wilson theory and describes phase separation.

When $\tilde{V}_{\text{co}}(k)$ assumes the global minimum $\tilde{V}_{\text{co}}(k_b)<0$ for $k=k_b\neq 0$, and can be expanded about $k=k_b$, then the truncated expansion

$$\tilde{V}_{\text{co}}(k) = \tilde{V}_{\text{co}}(k_b) + \tilde{V}_{\text{co}}^{(2)}(k_b)(k-k_b)^2/2 + \cdots \quad (66)$$

inserted in Eq. (58) yields $\tilde{C}_2^0(k)$ similar to the LB form (63). Truncation of the expansion of $\tilde{V}_{\text{co}}(k)$ is justified when the fields $\tilde{\rho}^*(\mathbf{k})$ with large $|\mathbf{k}-\mathbf{k}_b|$ yield negligible contribution to Ω. This is the case when the global minimum of $\tilde{V}_{\text{co}}$ is deep. In the following, we shall focus on systems with such forms of $\tilde{V}_{\text{co}}(k)$—they include weakly charged globular proteins, nanoparticles, colloids, or rigid micells in various solvents that mediate effective interaction potentials. Recall that in the mesoscopic theory, we choose the length scale R, and consequently introduce the cutoff π/R. The results of the Landau-Brazovskii theory describe actual ordering when the dominant contribution to Ω depends on k_b, but is independent of R.

E. Brazovskii-type approximation

Let us briefly summarize the original Brazovskii approximation, but with the coupling constants expressed in terms of physical quantities according to Eqs. (64), (58), and (66), and discuss conditions of its validity. The Brazovskii theory is particularly simple, and analytical results can be obtained easily. In the original Brazovskii theory, $\tilde{C}_2$ is calculated to first order in A_4, and is given by [20]

$$\tilde{C}_2(k) = \tilde{C}_2^{\text{co}}(k) + \frac{A_4}{2}\mathcal{G} = \tau + \beta^* v_2^*(k-k_b)^2, \quad (67)$$

where we simplify the notation by introducing

$$v_2^* = \frac{\tilde{V}_{\text{co}}^{(2)}(k_b)}{2|\tilde{V}_{\text{co}}(k_b)|} \quad (68)$$

and

$$\tau = \tilde{C}_2(k_b) = \tilde{C}_2^{\text{co}}(k_b) + \frac{A_4}{2}\mathcal{G}, \quad (69)$$

and where the dimensionless temperature is defined by

$$T^* = 1/\beta^* = \frac{k_B T}{-\tilde{V}_{\text{co}}(k_b)}. \quad (70)$$

$\tilde{C}_2^{\text{co}}(k)$ and $\mathcal{G}$ are given in Eqs. (58) and (53), respectively, and k_b corresponds to the minimum of $\tilde{V}_{\text{co}}$ [see the definition of V_{co} in Eq. (11)]. Note that Eq. (67) is consistent with our result (50) with $\bar{f}^{(4)}[\bar{\rho}^*]$ approximated by A_4, up to a correction that is of order A_4^2.

When the main contribution to $\mathcal{G}$ comes from $k\approx k_b$, the regularized integral (53) can be approximated by [20,38]

$$\mathcal{G} = \int_{\mathbf{k}} \frac{1}{\tilde{C}_2(k)} \simeq \int_{\mathbf{k}\in S_{\pi/R}} \frac{1}{\tau + \beta^* v_2^*(k-k_b)^2}. \quad (71)$$

The integral on the RHS of Eq. (71) can be calculated analytically [38]. In the case of $\tau \ll \beta^* v_2^* k_b^2$, $\mathcal{G}$ takes the asymptotic form

$$\mathcal{G} \simeq_{\tau\ll\beta^* v_2^* k_b^2} \mathcal{G}(\tau) + \frac{T^*}{2\pi v_2^* R} + O(\ln(\pi/R)), \quad (72)$$

where

$$\mathcal{G}(\tau) = \frac{2a\sqrt{T^*}}{\sqrt{\tau}} \tag{73}$$

and

$$a = k_b^2/(4\pi\sqrt{v_2^*}). \tag{74}$$

Note the independence of $\mathcal{G}(\tau)$ on the mesoscale R. In the Brazovskii theory, the R-dependent terms in Eq. (72) are neglected. The Brazovskii approximation

$$\mathcal{G} \simeq \mathcal{G}(\tau) \tag{75}$$

is valid when the second term in Eq. (72) is indeed negligible compared to the first term for $1 < R < \pi/k_b$, i.e.,

$$\tau \ll k_b^4 \beta^* v_2^*. \tag{76}$$

Note also that the original Brazovskii theory is restricted to $k \approx k_b$, because of the approximation (66). From Eqs. (69), (75), and (58), we obtain the explicit expression for $\tau = \tilde{C}_2(k_b)$,

$$\tau^{3/2} = \tau^{1/2}\tilde{C}_2^{\rm co}(k_b) + A_4 a\sqrt{T^*}. \tag{77}$$

The grand potential functional (54) in the Brazovskii approximation takes the explicit form

$$\beta\Omega[\bar{\rho}^* + \Phi] = \beta\Omega_{\rm co}[\bar{\rho}^* + \Phi] + 2a\sqrt{\tau T^*}V - \frac{A_4\mathcal{G}^2(\tau)}{8}V, \tag{78}$$

where τ satisfies Eq. (77), A_2 and A_4 are given in Eqs. (C1) and (C3), respectively, and $\beta\Omega_{\rm co}[\bar{\rho}^* + \Phi]$ in the Brazovskii-type approximation is given in Eq. (60). The second term in Eq. (78) is the explicit form of the second term in Eq. (54) for $\tilde{C}_2(k)$ given in Eq. (67) [22,36]. In calculating the third term on the RHS in Eq. (54), Eq. (67) was used. The above expression is valid provided that the condition (76) is satisfied.

The global minimum of the functional (78) with respect to Φ corresponds to the stable phase for given $\bar{\rho}_0^*$ and T^*. The problem of finding the minimum of Eq. (78) becomes easy for periodic structures of given symmetry. For given symmetry, $\Phi(\mathbf{r})$ can be written in the form

$$\Phi(\mathbf{r}) = \sum_n \Phi_n g_n(\mathbf{r}), \tag{79}$$

where $g_n(\mathbf{r})$ represent the orthonormal basis functions for the nth shell that have a particular symmetry, and satisfy the normalization condition

$$\frac{1}{V_u}\int_{\mathbf{r}\in\mathcal{V}_u} g_n(\mathbf{r})^2 = 1. \tag{80}$$

Φ_n is the nth amplitude. For given symmetry, the problem reduces to the determination of the minimum of the function of variables Φ_n.

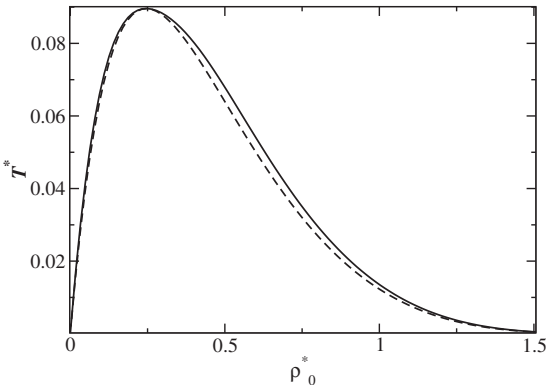

FIG. 2. Dashed line is the universal line (82). Solid line is the universal first-order transition line between the disordered and the bcc phases in the one-shell MF approximation. When $\tilde{V}_{\rm co}(k)$ assumes the global minimum for $k=0$, the dashed line represents the MF spinodal line of the gas-liquid separation. When $\tilde{V}_{\rm co}(k)$ assumes the global minimum for $k=k_b>0$, the dashed line represents the λ line associated with formation of ordered periodic phases. T^* and ρ_0^* are dimensionless temperature and density defined in Eqs. (70) and (12), respectively.

V. EXPLICIT RESULTS

A. Structure of the disordered phase and the λ line

Let us focus on the stability of the disordered phase. In the first step, let us limit ourselves to the MF approximation and consider stability of the functional $\Omega_{\rm co}$. When $\tilde{C}_2^{\rm co}(k) < 0$, then $\Omega_{\rm co}$ is unstable with respect to the density wave with the wave number k. At the boundary of stability, the second functional derivative of $\Omega_{\rm co}$ vanishes for $k=k_b$, i.e.,

$$\tilde{C}_2^{\rm co}(k_b) = 0, \tag{81}$$

since such instability occurs at the highest temperature for given density. In the PY approximation, the above equation yields together with Eqs. (58) and (C1) the *universal* curve

$$T_\lambda^*(\bar{\rho}_0^*) = \frac{\bar{\rho}_0^*(1-\eta)^4}{(1+2\eta)^2}, \tag{82}$$

where the dimensionless temperature is defined in Eq. (70) and $\tilde{V}_{\rm co}(k)$ assumes the global minimum, $\tilde{V}_{\rm co}(k_b) < 0$, for $k = k_b$. Universality in this context means that the shape of $\tilde{V}_{\rm co}(k)$ is irrelevant, and the value at the minimum, $\tilde{V}_{\rm co}(k_b)$, sets the temperature scale. For properly rescaled temperatures, the boundaries of stability of $\Omega_{\rm co}$ for all systems with particles having spherical cores collapse onto the single master curve (82).

For $k_b=0$, Eq. (82) represents the MF approximation for the spinodal line of the gas-liquid separation, whereas for $k_b \neq 0$ the above represents the λ line [31,33–35,38,39,45,46,49] associated with microsegregation. A similar result was obtained previously [41,45–48]. The universal line (82) is shown in Fig. 2 (dashed line).

Let us consider the actual boundary of stability of the uniform phase in the system in which $\tilde{V}_{\rm co}(k)$ assumes the global minimum for $k_b>0$. Beyond MF, the boundary of stability of the grand potential Ω is given by

$$\tilde{C}_2(k_b)=0. \tag{83}$$

In the Brazovskii theory, $\tilde{C}_2(k_b)=\tau$ satisfies Eq. (77). Equations (83) and (77) yield $T=0$ independently of density. This means that when $\tilde{V}_{\rm co}(k)$ assumes the global minimum for $k_b>0$, the MF boundary of stability with respect to periodic ordering, Eq. (82), is shifted down to zero temperature when the mesoscopic scale fluctuations are included. At the λ line, the structure factor $S(k)=\tilde{G}_2(k)/\bar{\rho}_0^*$ diverges for $k\to k_b$ for $\tilde{G}_2(k)$ approximated by $\tilde{G}_2^{\rm co}(k)=1/\tilde{C}_2^{\rm co}(k)$. In the Brazovskii approximation the maximum of the structure factor is finite at the λ line, and we obtain its value from Eqs. (77) and (81),

$$\tilde{G}_2(k_b)=1/\tau=\left[\frac{(4\pi)^2 v_2^* A_2}{k_b^4 A_4^2}\right]^{1/3}. \tag{84}$$

Recall that Eq. (77) is valid provided that τ satisfies the condition (76), which at the λ line takes the form

$$\frac{A_4}{A_2^2}\ll 4\pi(v_2^* k_b^2)^2. \tag{85}$$

For $\bar{\rho}_0^*\to 0$, the approximation (75) is not valid at the λ line, because the LHS of Eq. (85) behaves as $(\bar{\rho}_0^*)^{-1}$ (see Appendix C), whereas the RHS is independent of $\bar{\rho}_0^*$. The RHS of Eq. (85) depends on the system, therefore the density range for which the approximation (75) is valid at the λ line is system-dependent.

The infinite susceptibility with respect to periodic external field, resulting from singularity of the structure factor for finite k, is the artifact of the MF approximation. In the mesoscopic theory, the interpretation of the λ line follows from Eqs. (7) and (60). For $T^*<T_\lambda^*(\bar{\rho}_0)$ [i.e., $\tilde{C}_2^{\rm co}(k_b)<0$], the *single mesostate with periodic density*, with the wave number k_b and infinitesimal amplitude, *is more probable* than the *uniform mesostate*. Recall that the mesoscopic density $\rho(\mathbf{r})$ is equivalent to the set of microstates that satisfy Eq. (3). Thus, for $T^*<T^*(\bar{\rho}_0)$ the probability of occurrence of *any microscopic state with nonuniform density distribution* at the length scale π/k_b is larger than the probability of finding *any microscopic state with position-independent density* (3) on the length scale $R\sim\pi/k_b$.

When $\tilde{V}_{\rm co}(0)<0$, then both the λ line and the spinodal line are present and the temperature at the MF spinodal line is

$$T_s^*(\bar{\rho}_0^*)=T_\lambda^*(\bar{\rho}_0^*)\frac{\tilde{V}_{\rm co}(0)}{\tilde{V}_{\rm co}(k_b)}. \tag{86}$$

$T_s^*(\bar{\rho}_0^*)<T_\lambda^*(\bar{\rho}_0^*)$ when $\tilde{V}_{\rm co}(k)$ assumes the global minimum for $k_b>0$. Both lines were found in Refs. [45,46,48] for some forms of the interaction potential. In fact, there is a family of curves $T_\lambda^*(\bar{\rho}_0^*)\tilde{V}_{\rm co}(k)/\tilde{V}_{\rm co}(k_b)$ representing the MF instability with respect to density waves with the wave number k. All of them lie below the λ line when $k_b>0$, or below the spinodal line when $k_b=0$.

B. Case of weak ordering—Universal features of the MF phase diagram

Let us determine the global minimum of the functional $\beta\Omega_{\rm co}[\bar{\rho}_0^*+\Phi]$ with respect to $\Phi(\mathbf{r})$ [see Eq. (4)]. The minimum of the functional of the same formal structure as in Eq. (60) was calculated in different context in Refs. [20–22,50], and we shall not repeat the details of the calculation, which can be found in the above papers.

In this section, we shall limit ourselves to the one-shell approximation. This approximation is valid when $\tilde{V}_{\rm co}(k_b)\ll\tilde{V}_{\rm co}(k_{b2})$, where k_{b2} is the wave number in the second shell. For structures possessing different symmetries, the Fourier transform of g_1 in Eq. (79) has the form

$$\tilde{g}_1(\mathbf{k})=\frac{(2\pi)^d}{\sqrt{2n}}\sum_{j=1}^{n}[w\delta(\mathbf{k}-\mathbf{k}_b^j)+w^*\delta(\mathbf{k}+\mathbf{k}_b^j)], \tag{87}$$

where w^* is the complex conjugate of w, and $ww^*=1$. $2n$ is the number of vectors $\mathbf{k}_b^j$ in the first shell of the considered structure. The forms of $g_1(\mathbf{r})$ in real-space representation are given in Appendix D for the lamellar, hexagonal, bcc, and gyroid ($Ia3d$) structures. From Eq. (60), we obtain in the one-shell approximation

$$\begin{aligned}\beta\Delta\omega_{\rm co}(\Phi_1)&=\beta(\Omega_{\rm co}[\bar{\rho}^*+\Phi_1 g_1(\mathbf{r})]-\Omega_{\rm co}[\bar{\rho}^*])/V\\&=\frac{1}{2}\tilde{C}_2^0(k_b)\Phi_1^2+\frac{A_3\kappa_3}{3!}\Phi_1^3+\frac{A_4\kappa_4}{4!}\Phi_1^4,\end{aligned} \tag{88}$$

where the geometric factors characterizing different structures are given by

$$\kappa_n=\frac{1}{V_u}\int_{\mathbf{r}\in\mathcal{V}_u} g_1(\mathbf{r})^n. \tag{89}$$

Note that in the one-shell approximation, $\beta\Delta\omega_{\rm co}(\Phi_1)$ depends on $\tilde{V}_{\rm co}(k)$ only through the product $\beta\tilde{V}_{\rm co}(k_b)$ [see Eq. (58)], therefore the phase diagram in variables $\bar{\rho}_0^*$, T^* is universal. From the extremum condition

$$\frac{\partial\beta\Delta\omega_{\rm co}}{\partial\Phi_1}=\tilde{C}_2^0(k_b)\Phi_1+\frac{A_3\kappa_3}{2}\Phi_1^2+\frac{A_4\kappa_4}{3!}\Phi_1^3=0, \tag{90}$$

we obtain Φ_1 of the stable or the metastable phase. The stable phase corresponds to the lowest value of $\beta\Delta\omega_{\rm co}(\Phi_1)$ for given thermodynamic variables, where Φ_1 satisfies Eq. (90). The coexistence between different ordered phases takes place when the grand potentials (88) for these phases are equal. At the coexistence of the stable ordered phase with the disordered (uniform) phase,

$$\Delta\omega_{\rm co}(\Phi_1)=0. \tag{91}$$

The universal MF phase diagram obtained in this way in the one-shell approximation is shown in Fig. 3. For $A_3\neq 0$, the

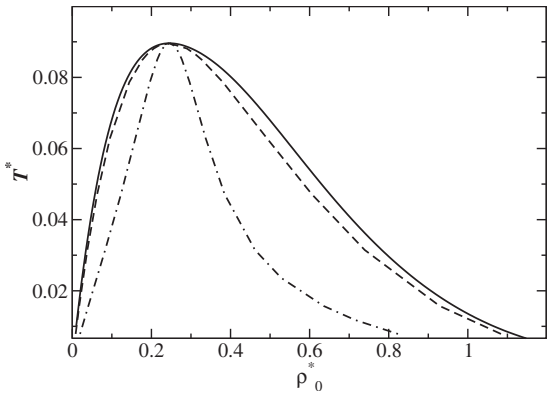

FIG. 3. MF phase diagram in the one-shell approximation. T^* and ρ_0^* are dimensionless temperature and density, Eqs. (70) and (12), respectively. Solid line is the coexistence of the uniform phase (above in T^*) and the bcc crystal. On the left from the maximum the bcc structure is formed by droplets (excess density), on the right by bubbles (depleted density). The bcc crystal coexists with the hexagonal structure along the dashed line. Again, on the left and on the right from the maximum the hexagonally packed cylinders consist of droplets and bubbles, respectively. The hexagonal phase coexists with the lamellar phase along the dash-dotted line.

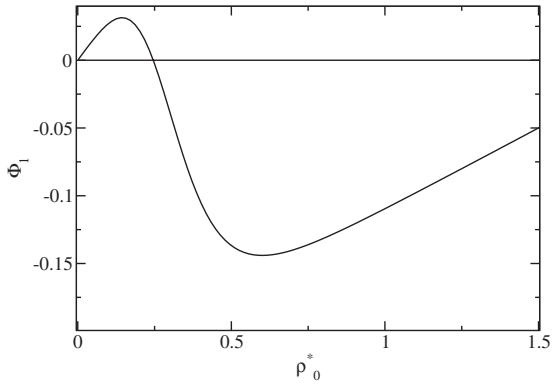

FIG. 4. The amplitude of the density profile $\bar{\rho}_0^*(\mathbf{r})=\bar{\rho}_0^*+\Phi_1 g_1^{\mathrm{bcc}}(\mathbf{r})$ in the bcc phase at the coexistence with the uniform phase (i.e., along the solid line in Fig. 3) in the one-shell MF approximation. Φ_1 and the space-averaged density $\bar{\rho}_0^*$ are both dimensionless.

ordered phase coexisting with the fluid has the bcc symmetry, and the uniform-bcc phase coexistence line is

$$T^*=\frac{3A_4\kappa_4^{\mathrm{bcc}}}{3A_4A_2\kappa_4^{\mathrm{bcc}}-(A_3\kappa_3^{\mathrm{bcc}})^2}, \tag{92}$$

as already shown by Leibler [50]. Explicit expressions for A_n are given in Appendix C, and the transition line (92) is shown in Fig. 2 together with the λ line, and in Fig. 3 together with transitions to the other phases. The lattice constant of the bcc phase is $a=2\sqrt{2}\pi/k_b$. Along the coexistence between the uniform and the bcc phases,

$$\Phi_1^{\mathrm{bcc}}=-\frac{16A_3}{15\sqrt{3}A_4}, \tag{93}$$

where the explicit forms of the geometric coefficients, $\kappa_3^{\mathrm{bcc}}=2/\sqrt{3}$ and $\kappa_4^{\mathrm{bcc}}=15/4$, were used. Φ_1^{bcc} at the transition to the uniform phase is independent of V_{co} and is shown in Fig. 4 for our PY form of f_h. For $A_3=0$, the transition is to the striped (lamellar) phase [50] and is continuous ($\Phi_1=0$). In our PY theory $A_3(\rho^*)=0$ for just one density $\rho^*=\rho_c^*$, where ρ_c^* is the maximum at the λ line, and at the same time the critical density of the gas-liquid separation. In the PY approximation (46), $\rho_c^*\approx 0.2457358$. Note that for densities lower than the gas-liquid critical-point density ρ_c^*, we obtain a periodic array of excess number density (cluster) forming the bcc crystal, whereas for higher densities the bcc structure is formed by bubbles of depleted density. Note also that $\Phi_1 \ll 1$ as required by the construction of the approximate theory (see Sec. III B).

The diagram shown in Fig. 3 is the universal "skeleton" showing the sequence of phases: disordered, bcc, hexagonal, lamellar, inverted hexagonal, inverted bcc, disordered. Note the reentrant melting at densities well below the close-packing density. The above sequence of phases agrees with the sequence observed for micellar solutions and block copolymers [28], and with the sequence of structures found in recent simulations for the SALR potential [44,46].

C. Example: The SALR potential in the case of very short range of attractions

Beyond the one-shell approximation, more complex structures can be stabilized, and we expect "decorations" of the universal skeleton diagram (Fig. 3) with regions of stability of more complex structures, or with structures with large amplitudes of the density oscillations. However, the diagrams are no longer universal, in the sense that the stability region of more complex structures depends not only on the value of $\beta\tilde{V}_{\mathrm{co}}(k_b)$, but also on $\beta\tilde{V}_{\mathrm{co}}(k_{bn})$, where k_{bn} is the wave number in the nth shell. Therefore, the details of the phase diagram depend on the shape of the interaction potential. Studies of the details of the phase diagrams in various systems go beyond the scope of this work. Just for illustration, we quote the results obtained for the SALR potential,

$$V_{\mathrm{SALR}}(r)=-A_a\frac{\exp(-z_1 r)}{r}+A_r\frac{\exp(-z_2 r)}{r}, \tag{94}$$

where r and z_i are in σ and $1/\sigma$ units, respectively, and the amplitudes are in k_BT_{room} units. The SALR potential describes in particular weakly charged colloids in a presence of short-chain nonadsorbing polymers inducing the depletion potential, globular proteins in some solvents, and rigid micelles. For the parameters $A_a=140e^{8.4}$, $A_r=30e^{1.55}$, $z_1=8.4$, and $z_2=1.55$, related to the colloid-polymer mixture [6], the Fourier transform of the potential $V_{\mathrm{co}}(r)=\theta(r-1)V_{\mathrm{SALR}}(r)$ is shown in Fig. 5 together with the approximation (66) that allows for the reduction to the Brazovskii theory. This potential leads to the formation of small clusters, because $k_b\approx 1.94$ in σ^{-1} units, and $2\pi/k_b\approx 3.24$. In Fig. 6, $\tilde{G}_2^{\mathrm{co}}(k)=S_{\mathrm{co}}(k)\bar{\rho}_0^*$, where $S_{\mathrm{co}}(k)$ is the structure factor in the MF approximation, is shown for $\bar{\rho}_0^*=\bar{\rho}_c^*\approx 0.246$ and $T^*=0.15$. The first peak corresponds to cluster-cluster correlations, as

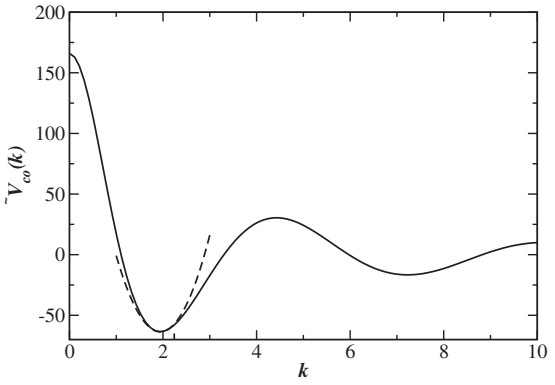

FIG. 5. The Fourier transform $\tilde{V}_{\rm co}(k)$ of $V_{\rm co}(r)=\theta(r-1)V_{\rm SALR}(r)$, where $V_{\rm SALR}(r)$ is the SALR potential (94) with $A_a=140e^{8.4}$, $A_r=30e^{1.55}$, $z_1=8.4$, and $z_2=1.55$ (solid line). Dashed line represents Eq. (66) that leads to the approximate Brazovskii theory. The minimum of $\tilde{V}_{\rm co}(k)$ is assumed at $k=k_b\approx 1.94$. The second-shell value for the gyroid phase, $k_{b2}=2k_b/\sqrt{3}$, is indicated on the k axis. $\tilde{V}_{\rm co}(k)$ and k are in $k_BT_{\rm room}$ and $1/\sigma$, units, respectively.

observed in simulations and experiments for the SALR systems [3,6,42,43,46]. The chosen thermodynamic state is away from the λ line, and $\tilde{G}_2^{\rm co}(k)$ is a reasonable approximation for the correlation function. When the λ line is approached, $\tilde{G}_2^{\rm co}(k_b)$ diverges and the MF approximation fails, as discussed in Sec. V A. In Fig. 7, $\tilde{G}_2(k_b)$ (maximum of the structure factor) is shown for $\bar{\rho}_0^*=\bar{\rho}_c^*\approx 0.246$ as a function of temperature for $T^*\leqslant T_\lambda^*(\bar{\rho}_c^*)$ in the Brazovskii approximation. In this case, the condition (76) is satisfied. We verified that inclusion of the second term in Eq. (72) with $R=1$ and $R=\pi/k_b$ leads to $\tilde{G}_2(k_b)\approx 0.14$ and $\tilde{G}_2(k_b)\approx 0.15$, respectively, at the λ line, while $\tilde{G}_2(k_b)\approx 0.16$ when the second term in Eq. (72) is neglected. Note that $\tilde{G}_2(k_b)$ assumes rather small values, in agreement with results obtained for ionic systems [38].

We find the diagram shown in Fig. 8 by calculating $\beta\Delta\omega_{\rm co}$ for the gyroid phase in the two-shell approximation. In this phase, the second shell is very close to the first shell ($k_{b2}=2k_b/\sqrt{3}$), unlike in the case of the other phases ($k_{b2}=\sqrt{2}k_b$, $k_{b2}=\sqrt{3}k_b$, and $k_{b2}=2k_b$ for the bcc, hexagonal, and lamellar phase, respectively). For this reason, the second shell in Eq. (79) should be included in the case of the gyroid phase, as argued in Ref. [22]. The details of the calculation will be given elsewhere along with the results obtained within the present mesoscopic theory beyond MF [40]. The unit cell of the gyroid phase is shown in Fig. 9 for $\bar{\rho}_0^*=0.048$ and $T^*=0.016$. Note that in this approximation, we obtain for low enough temperatures the sequence of phases: disordered-bcc-hexagonal-gyroid-lamellar-inverted gyroid-inverted hexagonal-inverted bcc-disordered. Such a sequence of phases is found in many self-assembling systems, including micellar systems and block copolymers. The bicontinuous cubic phase is usually found between the hexagonal and the lamellar phases. In simulations of the SALR potential, hexagonal and lamellar phases were found for similar densi-

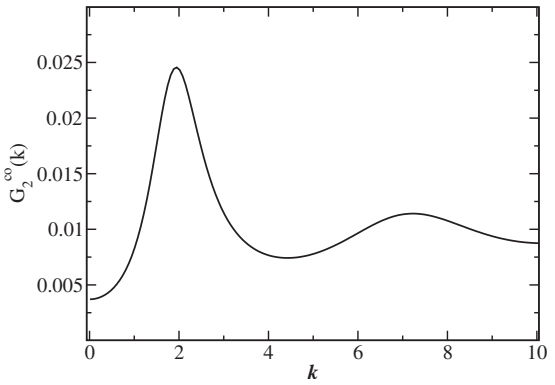

FIG. 6. $\tilde{G}_2^{\rm co}(k)=S_{\rm co}(k)\bar{\rho}_0^*$ for the SALR potential (94) with $A_a=140e^{8.4}$, $A_r=30e^{1.55}$, $z_1=8.4$, and $z_2=1.55$ for $\bar{\rho}_0^*=\bar{\rho}_c^*\approx 0.246$ and $T^*=0.15$.

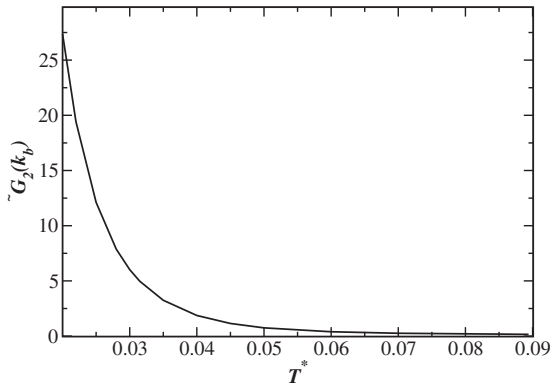

FIG. 7. $\tilde{G}_2(k_b)=1/\tau$, corresponding to the maximum of the structure factor, in the Brazovskii approximation (77), for $\bar{\rho}_0^*=\bar{\rho}_c^*\approx 0.246$ as a function of T^*.

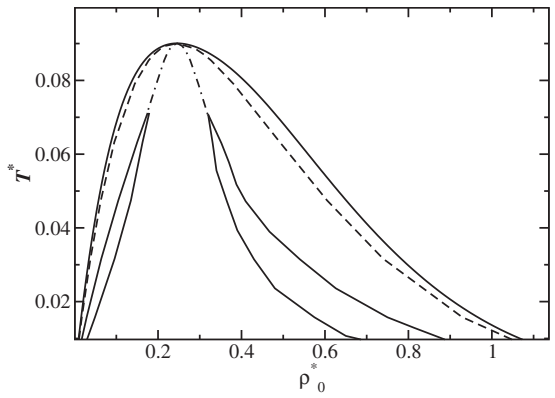

FIG. 8. MF phase diagram with the gyroid phase ($Ia3d$ symmetry) considered in the two-shell approximation, and the remaining phases in the one-shell approximation, as in Ref. [22]. The interaction potential has the SALR form (94) with $A_a=140e^{8.4}$, $z_1=8.4$, $A_r=30e^{1.55}$, and $z_2=1.55$. The potential is chosen for the system consisting of charged colloids in the presence of small polymers, similar to the system studied experimentally in Ref. [6]. The diagram is the same as in Fig. 4 except that the $Ia3d$ phase is stable in the windows between the hexagonal and the lamellar phases. The structure of the phase in the left window is shown in Fig. 9. For more details, see Ref. [40].

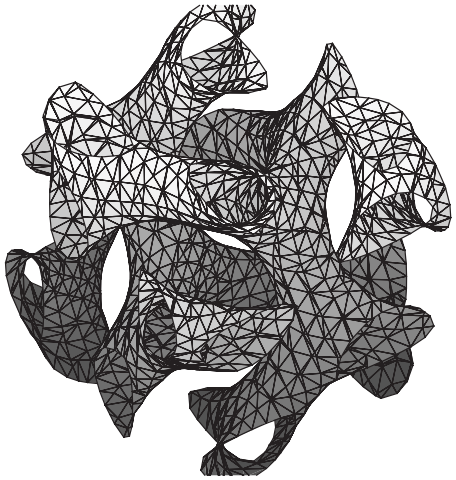

FIG. 9. The unit cell of the $Ia3d$ phase in the two-shell approximation for $\bar{\rho}_0^*=0.048$ and $T^*=0.016$. In the region enclosed by the shown surface, $\bar{\rho}^*(\mathbf{r})-\bar{\rho}_0^* \geqslant 0.06$, i.e., this surface shows the shape of the cluster of colloids. Note that two networks of branching regions of excess density are present in the two-shell approximation in the structure corresponding to the minimum of $\beta\Delta\omega_{\mathrm{co}}$. The lattice constant of the cubic unit cell is $2\pi\sqrt{6}/k_b \approx 8\sigma$. For more details, see Ref. [40].

ties as we predict; the inverted structures were not found for the considered density range [44]. In different simulations [46], spherical, cylindrical, and slablike liquidlike clusters were found for increasing density, and for $\bar{\rho}^* > 0.35$ cylindrical and next spherical bubbles were seen [46] for densities that agree with our predictions. The unit cell in this system contains too many particles to enable observation of the ordered phases. In colloid-polymer mixtures, spherical clusters, elongated clusters, and a network-forming cluster were observed experimentally for increasing volume fraction of colloids [6]. The relation between the experimentally observed (presumably metastable) structures and our results obtained for thermal equilibrium requires further studies.

VI. SUMMARY

We developed a formalism that has a form of the density-functional theory with an additional term in which the effect of the mesoscopic scale fluctuations is included. The theory is designed for studies of self-assembling systems, where nonuniform density distributions are found on the mesoscopic length scale λ, and allows for obtaining phase diagrams and structure in terms of density, temperature, and the (effective) interaction potentials. We present the grand-potential functional and the equations for the correlation functions starting from the most general form [Eqs. (24) and (27)]. In further development of the theory, higher-order correlations for the mesoscopic density are neglected, and the pair-correlation function satisfies Eq. (30). In Sec. IV, we derive an approximate version of the theory under the assumption $\lambda \gg \sigma$. The grand-potential functional and the equation for the correlation function on the mesoscale are given in Sec. IV B [Eqs. (50)–(54)]. These new equations allow for numerical determination of the structure and phase behavior in many self-assembling system with spherically symmetric interaction potentials. The theory can be generalized to nonspherical cores. Unlike in the standard DFT, the effects of mesoscopic fluctuations, leading in particular to fluctuation-induced first-order phase transition, are included. Unlike in the phenomenological LGW or LB theories, microscopic degrees of freedom are not disregarded in our theory, therefore it allows for predictions of structure and phase diagram in terms of temperature and density for given interaction potential. Equations (50)–(54) are not restricted to weak ordering.

We also show that in the case of weak ordering, our theory can be reduced to the form similar to either the LGW or the LB theory, depending on the interaction potential, and we derive the microscopic expressions for the coupling constants. This approximate version of the theory allows for analytical calculations; its validity range is discussed in detail in Sec. IV D.

In Sec. V, universal properties of self-assembly are determined in the framework of the mesoscopic theory introduced in Secs. IV C and IV E. We determine the λ line and conclude that it is related to structural changes in the disordered system. It is interesting that in the reduced units, the λ line and the MF spinodal line are given by the same universal curve (82).

In Sec. V B, we obtain the universal "skeleton" diagram (Fig. 3) with the universal sequence of ordered phases that agrees with many experimental observations in a wide class of self-assembling systems, and with simulation studies for the SALR potential [44,46]. This universal skeleton is "decorated" in particular systems with more complex structures, and modified by fluctuations, especially for high temperatures. By considering the gyroid phase for a particular form of the SALR potential in the two-shell approximation, we find in Sec. V C that this phase is stable between the hexagonal and lamellar phases for low enough temperatures (Fig. 8). As far as we know, there are no theoretical predictions (except from simulations that are incomplete) for the phase transitions between periodic phases in the three-dimensional system with the SALR interaction potential. The results of recent studies [47,48] are limited to the lamellar phase in three dimensions and to more complex structures in two dimensions.

The bicontinuous phase can be considered as a regular gel. The relation between this phase and the experimentally observed gels in colloid-polymer mixtures [6] is an interesting question. If the gyroid phase is thermodynamically stable, the gel observed in experiments may result from arrested microsegregation, and its structure should be more regular than the structure that is formed by arrested spinodal decomposition into two uniform phases. In particular, triple junctions of the cylindrical colloidal clusters should dominate.

ACKNOWLEDGMENTS

I would like to thank Dr. A. Archer for discussions and for sending us unpublished work (Refs. [47,48]). This work was partially supported by the Polish Ministry of Science and Higher Education, Grant No. NN 202 006034.

APPENDIX A: TWO-POINT VERTEX FUNCTION IN FOURIER REPRESENTATION IN THE CASE OF PERIODIC STRUCTURES

For periodic structures with the unit cell $\mathcal{V}_u$ of the volume V_u, with the structure invariant with respect to translations by the vector $\mathbf{P}=\Sigma_i^3 n_i\mathbf{p}_i$, where n_i are integer and the vectors $\mathbf{p}_i$ span the unit cell, we have

$$\begin{aligned}\tilde{\mathcal{C}}_2(\mathbf{k},\mathbf{k}+\mathbf{k}') &= \int_{\mathbf{r}_1}\int_{\mathbf{r}_2} \mathcal{C}_2(\mathbf{r}_1-\mathbf{r}_2|\mathbf{r}_2)e^{i\mathbf{k}\cdot(\mathbf{r}_1-\mathbf{r}_2)}e^{i(\mathbf{k}+\mathbf{k}')\cdot\mathbf{r}_2}\\ &= V_u\sum_{\mathbf{P}} e^{i(\mathbf{k}+\mathbf{k}')\cdot\mathbf{P}}\frac{1}{V_u}\int_{\mathbf{r}_2\in\mathcal{V}_u} e^{i(\mathbf{k}+\mathbf{k}')\cdot\mathbf{r}_2}\\ &\quad\times\int_{\mathbf{r}_1-\mathbf{r}_2} e^{i\mathbf{k}\cdot(\mathbf{r}_1-\mathbf{r}_2)}\mathcal{C}_2(\mathbf{r}_1-\mathbf{r}_2|\mathbf{r}_2)\\ &= (2\pi)^3\delta(\mathbf{k}+\mathbf{k}')\int_{\mathbf{r}_1-r_2} e^{i\mathbf{k}\cdot(\mathbf{r}_1-r_2)}\\ &\quad\times\frac{1}{V_u}\int_{\mathbf{r}_2\in\mathcal{V}_u}\mathcal{C}_2(\mathbf{r}_1-\mathbf{r}_2|\mathbf{r}_2).\end{aligned} \tag{A1}$$

Hence, we can write

$$\tilde{\mathcal{C}}_2(\mathbf{k},\mathbf{k}+\mathbf{k}') = (2\pi)^3\delta(\mathbf{k}+\mathbf{k}')\tilde{C}_2(\mathbf{k}), \tag{A2}$$

where

$$\tilde{C}_2(\mathbf{k}) = \int_{\Delta\mathbf{r}} C_2(\Delta\mathbf{r})e^{i\mathbf{k}\cdot\Delta\mathbf{r}}. \tag{A3}$$

APPENDIX B: EXPLICIT FORMS OF $\mathcal{C}_n^{\mathrm{co}}$ FOR PERIODIC STRUCTURES IN THE LOCAL-DENSITY APPROXIMATION

From Eq. (48), we obtain

$$\begin{aligned}&\mathcal{C}_1^{\mathrm{co}}[\bar{\rho}_0^*,\Phi,\mathbf{r}_1]\\ &= \beta\left[f_h^{(1)}(\bar{\rho}_0^*)+f_h^{(2)}(\bar{\rho}_0^*)\Phi(\mathbf{r}_1)+\frac{f_h^{(3)}(\bar{\rho}_0^*)}{2}\Phi(\mathbf{r}_1)^2\right.\\ &\quad\left.+\frac{f_h^{(4)}(\bar{\rho}_0^*)}{3!}\Phi(\mathbf{r}_1)^3-\mu+\int_{\mathbf{r}_2} V_{\mathrm{co}}(r_{12})[\bar{\rho}_0^*+\Phi(\mathbf{r}_2)]\right],\end{aligned} \tag{B1}$$

$$\begin{aligned}&\mathcal{C}_2^{\mathrm{co}}[\bar{\rho}_0^*,\Phi,\mathbf{r}_1,\mathbf{r}_2]\\ &= \beta\left[\left(f_h^{(2)}(\bar{\rho}_0^*)+f_h^{(3)}(\bar{\rho}_0^*)\Phi(\mathbf{r}_1)+\frac{f_h^{(4)}(\bar{\rho}_0^*)}{2}\Phi(\mathbf{r}_1)^2\right)\right.\\ &\quad\left.\times\delta(\mathbf{r}_1-\mathbf{r}_2)+V_{\mathrm{co}}(r_{12})\right],\end{aligned} \tag{B2}$$

$$\mathcal{C}_3^{\mathrm{co}}[\bar{\rho}_0^*,\Phi,\mathbf{r}] = \beta[f_h^{(3)}(\bar{\rho}_0^*)+f_h^{(4)}(\bar{\rho}_0^*)\Phi(\mathbf{r})], \tag{B3}$$

$$\mathcal{C}_4^{\mathrm{co}}[\bar{\rho}^*,\Phi] = \beta f_h^{(4)}(\bar{\rho}_0^*). \tag{B4}$$

APPENDIX C: EXPRESSIONS FOR THE COUPLING CONSTANTS A_n IN THE PY APPROXIMATION

The explicit forms of $A_n=\beta f_h^{(n)}(\bar{\rho}_0^*)$, for f_h approximated by Eq. (46), are

$$A_2 = \frac{(1+2\eta)^2}{(1-\eta)^4\bar{\rho}_0^*}, \tag{C1}$$

$$A_3 = \frac{12\eta^3+20\eta^2+5\eta-1}{(1-\eta)^5\bar{\rho}_0^{*2}}, \tag{C2}$$

$$A_4 = \frac{2-12\eta+30\eta^2+112\eta^3+48\eta^4}{(1-\eta)^6\bar{\rho}_0^{*3}}. \tag{C3}$$

APPENDIX D: $g_1(\mathbf{r})$ FOR SEVERAL STRUCTURES

The function $g_1(\mathbf{r})$ is given for the lamellar, hexagonal, bcc, and gyroid phases in Eqs. (D1)–(D4), respectively, with $\mathbf{r}=(x_1,x_2,x_3)$. The minimum of $\tilde{V}_{\mathrm{co}}(k)$ corresponds to k_b,

$$g_1^{\ell}(\mathbf{r}) = \sqrt{2}\cos(k_b x_1), \tag{D1}$$

$$g_1^{\mathrm{hex}}(\mathbf{r}) = \sqrt{\frac{2}{3}}\left[\cos(k_b x_1)+2\cos\left(\frac{k_b x_1}{2}\right)\cos\left(\frac{\sqrt{3}k_b x_2}{2}\right)\right], \tag{D2}$$

$$g_1^{\mathrm{bcc}}(\mathbf{r}) = \frac{1}{\sqrt{3}}\sum_{i<j}\left(\cos\left(\frac{k_b(x_i+x_j)}{\sqrt{2}}\right)+\cos\left(\frac{k_b(x_i-x_j)}{\sqrt{2}}\right)\right), \tag{D3}$$

$$\begin{aligned}g_1^{\mathrm{giro}}(\mathbf{r}) = \sqrt{\frac{8}{3}}\left[\right.&\cos\left(\frac{k_b x_1}{\sqrt{6}}\right)\sin\left(\frac{k_b x_2}{\sqrt{6}}\right)\sin\left(\frac{2k_b x_3}{\sqrt{6}}\right)\\ &+\cos\left(\frac{k_b x_2}{\sqrt{6}}\right)\sin\left(\frac{k_b x_3}{\sqrt{6}}\right)\sin\left(\frac{2k_b x_1}{\sqrt{6}}\right)\\ &\left.+\cos\left(\frac{k_b x_3}{\sqrt{6}}\right)\sin\left(\frac{k_b x_1}{\sqrt{6}}\right)\sin\left(\frac{2k_b x_2}{\sqrt{6}}\right)\right].\end{aligned} \tag{D4}$$

[1] M. Seul and D. Andelman, Science **267**, 476 (1995).
[2] W. M. Gelbart, R. P. Sear, J. R. Heath, and S. Chaney, Faraday Discuss. **112**, 299 (1999).
[3] A. Stradner, H. Sedgwick, F. Cardinaux, W. Poon, S. Egelhaaf, and P. Schurtenberger, Nature **432**, 492 (2004).
[4] H. Sedgwick, S. Egelhaaf, and W. Poon, J. Phys.: Condens. Matter **16**, S4913 (2004).
[5] R. Sanchez and P. Bartlett, J. Phys.: Condens. Matter **17**, S3551 (2005).
[6] A. I. Campbell, V. J. Anderson, J. S. van Duijneveldt, and P. Bartlett, Phys. Rev. Lett. **94**, 208301 (2005).
[7] E. Stiakakis, G. Petekidis, V. D, C. N. Likos, H. Iatrou, N. Hadjichristidis, and J. Roovers, Europhys. Lett. **72**, 664 (2005).
[8] N. Hoffmann, F. Ebert, C. N. Likos, H. Lowen, and G. Maret, Phys. Rev. Lett. **97**, 078301 (2006).
[9] V. A. Andreev and A. I. Victorov, Mol. Phys. **105**, 239 (2007).
[10] A. K. Arora and B. V. R. Tata, Adv. Colloid Interface Sci. **78**, 49 (1998).
[11] T. Konishi and N. Ise, Phys. Rev. B **57**, 2655 (1998).
[12] A. Ciach and W. T. Góźdź, Annu. Rep. Prog. Chem., Sect. C: Phys. Chem. **97**, 269 (2001), and references therein.
[13] N. Ise, T. Konish, and B. Tata, Langmuir **15**, 4176 (1999).
[14] P. C. Royall, M. E. Leunissen, A.-P. Hynninen, M. Dijkstra, and A. van Blaaderen, J. Chem. Phys. **124**, 244706 (2006).
[15] D. Pini, G. Stell, and N. B. Wilding, Mol. Phys. **95**, 483 (1998).
[16] R. Evans, Adv. Phys. **28**, 143 (1979).
[17] D. Pini, A. Parola, and L. Reatto, J. Phys.: Condens. Matter **18**, S2305 (2006).
[18] J. Zinn-Justin, *Quantum Field Theory and Critical Phenomena* (Clarendon, Oxford, 1989).
[19] D. J. Amit, *Field Theory, the Renormalization Group and Critical Phenomena* (World Scientific, Singapore, 1984).
[20] S. A. Brazovskii, Sov. Phys. JETP **41**, 8 (1975).
[21] G. H. Fredrickson and E. Helfand, J. Chem. Phys. **87**, 697 (1987).
[22] V. E. Podneks and I. W. Hamley, Pis'ma Zh. Eksp. Teor. Fiz. **64**, 564 (1996).
[23] I. Yukhnovskii, Sov. Phys. JETP **34**, 263 (1958).
[24] I. R. Yukhnovskii, *Phase Transitions of the Second Order, Collective Variable Methods* (World Scientific, Singapore, 1978).
[25] J. M. Caillol, O. Patsahan, and I. Mryglod, Physica A **368**, 326 (2006).
[26] A. Parola and L. Reatto, Phys. Rev. A **31**, 3309 (1985).
[27] A. Parola and L. Reatto, Adv. Phys. **44**, 211 (1995).
[28] G. Fredrickson, V. Ganesan, and F. Drolet, Macromolecules **35**, 16 (2002).
[29] M. Mueller, K. Katsov, and M. Schick, Phys. Rep. **434**, 113 (2006).
[30] A. Ciach, W. T. Góźdź, and G. Stell, J. Phys.: Condens. Matter **18**, 1629 (2006).
[31] A. Ciach and G. Stell, J. Mol. Liq. **87**, 255 (2000).
[32] A. Ciach and G. Stell, J. Chem. Phys. **114**, 382 (2001).
[33] A. Ciach and G. Stell, J. Chem. Phys. **114**, 3617 (2001).
[34] A. Ciach and G. Stell, Phys. Rev. Lett. **91**, 060601 (2003).
[35] A. Ciach, W. T. Góźdź, and R. Evans, J. Chem. Phys. **118**, 3702 (2003).
[36] A. Ciach, Phys. Rev. E **73**, 066110 (2006).
[37] A. Ciach and O. Patsahan, Phys. Rev. E **74**, 021508 (2006).
[38] O. Patsahan and A. Ciach, J. Phys.: Condens. Matter **19**, 236203 (2007).
[39] A. Ciach, W. T. Góźdź, and G. Stell, Phys. Rev. E **75**, 051505 (2007).
[40] A. Ciach and W. T. Góźdź (unpublished).
[41] R. P. Sear and W. M. Gelbart, J. Chem. Phys. **110**, 4582 (1999).
[42] F. Sciortino, S. Mossa, E. Zaccarelli, and P. Tartaglia, Phys. Rev. Lett. **93**, 055701 (2004).
[43] F. Sciortino, P. Tartaglia, and E. Zaccarelli, J. Phys. Chem. B **109**, 21942 (2005).
[44] A. de Candia, E. DelGado, A. Fierro, N. Sator, M. Tarzia, and A. Coniglio, Phys. Rev. E **74**, 010403(R) (2006).
[45] A. J. Archer, D. Pini, R. Evans, and L. Reatto, J. Chem. Phys. **126**, 014104 (2007).
[46] A. J. Archer and N. B. Wilding, Phys. Rev. E **76**, 031501 (2007).
[47] A. J. Archer, Phys. Rev. E **78**, 031402 (2008).
[48] A. Archer, C. Ionescu, D. Pini, and L. Reatto, J. Phys.: Condens. Matter **20**, 415106 (2008).
[49] G. Stell, *New Approaches to Problems in Liquid-State Theory* (Kluwer Academic, Dordrecht, 1999).
[50] L. Leibler, Macromolecules **13**, 1602 (1980).